EUROPEAN ORGANIZATION FOR NUCLEAR RESEARCH

Proposal to the ISOLDE and Neutron Time-of-Flight Committee

^{18}N: a challenge to the shell model and a part of the flow path to r-process element production in Type II supernovae

May 29, 2013

A. Matta[1], W.N. Catford[1], N.K. Timofeyuk[1], N.L. Achouri[2], S. Bönig[3], F. Delaunay[2], B. Fernandez-Dominguez[4], F. Flavigny[5], S.J. Freeman[6], J. Gibelin[2] , S. Ilieva[3], D.G. Jenkins[7], T. Kröll[3] M. Labiche[8], D. Mücher[9], N. Orr[2], G. Randisi[5], M. Thürauf[3], G.L. Wilson[1,7] with the T-REX and MINIBALL collaborations

[1] *Department of Physics, University of Surrey, Guildford, Surrey, GU2 7XH, UK*
[2] *LPC Caen, ENSICAEN, Caen,14050, France*
[3] *Institut für Kernphysik, Technische Universität Darmstadt, Darmstadt D-64289, Germany*
[4] *Universidad Santiago de Compostela, Santiago de Compostela,15782, Spain*
[5] *Instituut voor Kern- en Stralingsfysica, KU Leuven,Heverlee, B-3001, Belgium*
[6] *The School of Physics and Astronomy, University of Manchester, Manchester, M13 9PL, UK*
[7] *Department of Physics, University of York, York, YO10 5DD, UK*
[8] *STFC Daresbury Laboratory, Daresbury, Warrington, Cheshire, WA4 4AD, UK*
[9] *Physik-Department,Technische Universität München, Garching, 85748, Germany*

Spokespersons:
A. Matta (a.matta@surrey.ac.uk) and W.N. Catford (w.catford@surrey.ac.uk)
Contact person:
E. Rapisarda (elisa.rapisarda@cern.ch)

Abstract: We propose a study of the spectroscopy of ^{18}N using the (d,p) reaction at 5.5 Mev/A in inverse kinematics with the T-REX array and Miniball. The proton angular distributions measured using T-REX will allow us to deduce the orbitals and spectroscopic strengths associated with the bound and unbound excited states in ^{18}N. The measurement of coincident gamma rays will assist in resolving and determining the precise excitation energies for bound states in ^{18}N.

Requested shifts: 30 shifts

1 Previous experimental program and achievements

This experiment forms a natural part of our established programme to study neutron rich light nuclei via single-neutron transfer. In a a series of studies [1, 2, 3, 4], we have addressed the evolution of the neutron magic numbers which sees the classical magic numbers of $N = 20$ and 28 replaced by $N = 16$. An important theme has been the relative rise in energy of states based on the $0d_{3/2}$ orbital for neutron-rich nuclei. This is also important in considering ^{18}N, where the strong states of this structure are predicted to lie in the low-energy neutron resonance region. Also at GANIL, we previously studied the interaction of $0p$-shell protons with sd-shell neutrons in ^{12}Be [5] and we are preparing to study ^{17}C via the (d,p) reaction [6]. The techniques in our previous (d,p) studies are exactly those that we propose to apply at HIE-ISOLDE using T-REX and MINIBALL. The best choice for this experiment is T-REX since it has been established as a standard piece of equipment to be operated with MINIBALL. The beam intensities that we have used at SPIRAL match the intensity that we anticipate for ^{17}N, and we have used energies of both 5 and 10 MeV/A.

2 Motivations

2.1 Structure

The present state of knowledge of bound states in ^{18}N is summarised in Fig.1 and compared with ^{18}Na from ^{17}Ne+p [7]. Note that the second doublet in ^{18}N is labelled (0^-), (1^-) as suggested in the original study [8]. The two states 0^-_1 and 2^-_2 are then almost degenerate. Similarly the 1^-_2 and 3^-_1 states are almost degenerate. The NNDC data base misassigns the 0^- and 1^- states [9]. However the arguments for the all four states are strong and can be understood in terms of the reaction selectivity. The experimental spectrum of ^{18}N is compared in Fig. 2 to two published shell model calculations [10] and our *spsdpf* calculations with NuShell [11] using the WBP interaction. None of the shell model calculations can reproduce the ordering of the two low-lying states and the deviations from the experimental energies are as high as 400 keV, which is larger than the typical 100 keV. In addition, the WBP calculations predict many bound positive parity states which are absent in the experimental spectrum. Such deviations reflect poorly understood features of the $\pi(p_{1/2}) \otimes \nu(sd)$ coupling or of the evolution of nuclear levels in odd-odd nuclei with increasing neutron excess. The present experiment can clarify this.

2.2 Astrophysics

In a viable scenario of the r-process in neutrino-driven winds, the initial condition is a high-entropy hot plasma consisting of neutrons, protons and electron-positron pairs experiencing an intense flux of neutrinos. It has been shown by Terasawa *et al* [12] that in such an environment light nuclei, as well as heavy nuclei, play important roles in the production of seed nuclei and r-process elements. They have found that a new nuclear reaction flow path opens in the very light neutron-rich region that can change the final heavy-element abundances by as much as an order of magnitude (see Fig. 3). The new

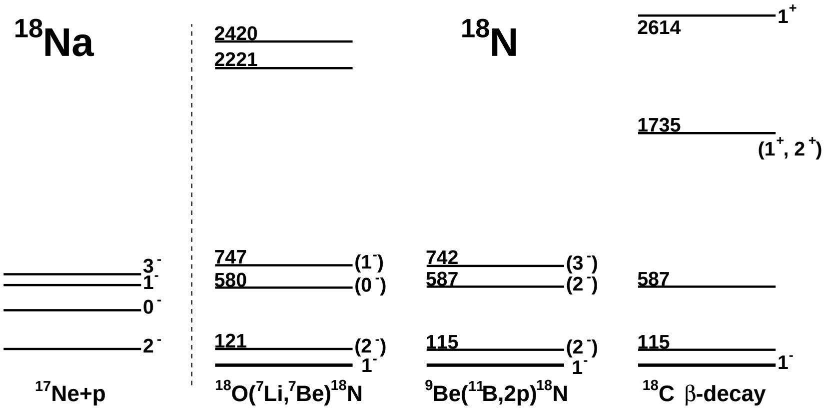

Figure 1: ^{18}N *level schemes from previous experiments in comparison to the* ^{18}Na *spectrum. For the various experiments, we include only the spin information that is discussed in that particular work. For* ^{18}Na*, the first* 2^- *is plotted at the position of the first* 2^- *in* ^{18}N *states observed in [8] and the spacings between all the* ^{18}N *states are to scale.*

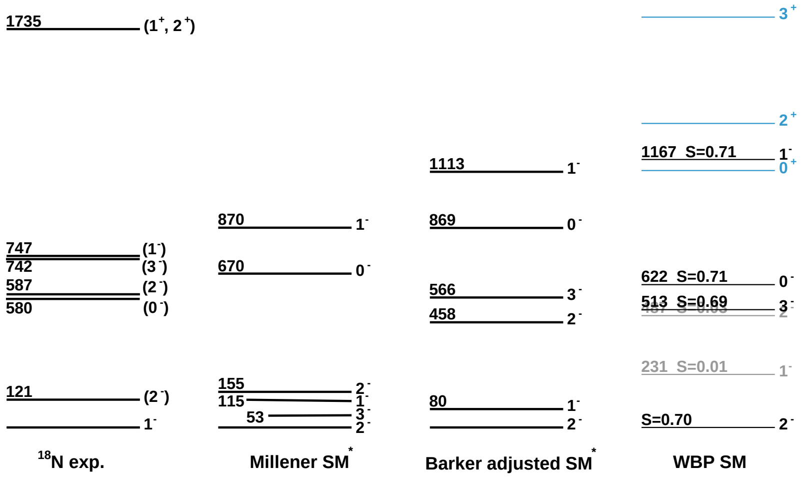

Figure 2: *Comparison of the experimental level scheme in* ^{18}N *(in our interpretation) with the shell model. For the WBP SM calculations, the spectroscopic factors of negative-parity states are also included. The neutron separation energy is 2.825 MeV. *Ref.[10]*

E (keV)	J^π	$S_{1s_{1/2}}$	$S_{0d_{3/2}}$	$S_{0d_{5/2}}$	E (keV)	J^π	$S_{1p_{1/2}}$	$S_{1p_{3/2}}$	$S_{0f_{5/2}}$	$S_{0f_{7/2}}$
0	2^-_1		0.0004	0.6997	1119	0^+_1	0.0037			
231	1^-_1	0.0054	0.0118		1324	2^+_1		0.0005	0.0005	
487	2^-_2		0.0324	0.0012	1787	3^+_1			0.0002	0.0013
513	3^-_1			0.6890	1855	1^+_1	0.0051	0.0033		
622	0^-_1	0.7148			2511	2^+_2		0.0034	0.0053	
1167	1^-_2	0.7051	0.0104		2692	1^+_2	0.0004	0.0050		
2240	2^-_3		0.0001	0.0216	2781	4^+_1				0.0031
2545	3^-_2			0.0023						

Table 1: *Spectroscopic factors from the ground state of* ^{17}N *for negative parity (left) and positive parity (right) bound states in* ^{18}N *as given by our spsdpf shell model calculations.*

reaction network requires more than 63 nuclides for $Z < 10$ with more than 200 reactions among them. In particular, it includes (n,γ) reactions on neutron-rich short-lived nitrogen isotopes. The abundances of nitrogen isotopes increase with the neutron number reaching its maximum at ^{23}N for the typical time of 0.57 s for the r-process (see Fig. 4) [12].
The nuclear reaction rates employed for the nucleosynthesis study in the neutrino wind model by Terasawa *et al* [12] and in a more recent work by Sasaqui *et al* [13] were taken from compilations dating from 1975 and 1988 when no information on reactions with unstable nuclei was available. The information about individual reaction rates becomes important when the nucleon separation energy of the synthesized level is larger than the temperature of the environment. This is definitely the case for the ^{18}N levels expected to be produced in supernovae as their neutron separation energies are larger than 2 MeV. We are aware of only one work (published in 1999) in which (n,γ) rates for nitrogen isotopes were calculated using spectroscopic factors obtained from a contemporary version of the shell model [14]. In these calculations the experimental excitation energies for the 2_1^- and 3_1^- states were used but the 1_2^- level was assumed to be unjustifiably high. Also, the shell model of ref.[14] predicts many resonance levels in the Gamow window and suggests that the ^{17}N(n,γ)^{18}N rate can be more than an order or magnitude larger than the Hauser-Feschbach predictions that are often used in nucleosynthesis calculations.
The previous experimental work on ^{18}N fails to provide satisfactory information on the states of interest for the radiative capture from ^{17}N. The (d,p) reaction mechanism is the tool of choice for such a study as it naturally selects the states of importance for radiative capture. The angular distributions of the populated states will provide clear assignment of their spins and the essential information for calculating the nuclear reaction rate in the stellar environment, mainly dominated by *s*- and *p*-waves. By extracting spectroscopic factors and asymptotic normalization coefficients, we will predict the ^{17}N(n,γ)^{18}N cross sections for the future needs of supernova calculations. The opportunity to populate resonances above the neutron emission threshold and measure them using missing mass methods is a key feature of the proposed experiment. It will clarify the mechanism of ^{17}N(n,γ)^{18}N capture at supernovae temperatures.

2.3 Selectivity of the (d,p) reaction

Which of the ^{18}N states should be populated in the (d,p) reaction? Firstly, the 2_1^- and 3_1^- can be populated. As discussed by Putt [8], the shell model of Millener indicates that these have a structure of $\pi(0p_{1/2})^{-1}$ coupled to $\nu(^{19}\mathrm{O}\ \frac{5}{2}^+)$ and can be populated by adding a neutron to the pair already coupled to spin zero in $0d_{5/2}$ in ^{17}N. The ground state 1_1^- and 2_2^- states are $\pi(0p_{1/2})^{-1}\otimes\nu(^{19}\mathrm{O}\ \frac{3}{2}^+)$ and will be suppressed as they require a recoupling of the $0d_{5/2}$ neutrons. The 0_1^- and 1_2^- should be strongly populated via transfer of a neutron to the $1s_{1/2}$ orbital. Our full shell model calculations support all of these expectations (see Tab.1 for spectroscopic factor calculations).
Thus, via (d,p) we can populate both states in the 742/747 keV doublet of $3^-/1^-$ and the 0^-state around 580 keV (cf. figure 2). There may be weak population also of the 587 keV 2^- state. In addition, the 121 keV 2^- state should be populated. It may be possible to determine lifetime information by the shadowing technique for this state (which is measured as $\tau = 0.58 \pm 0.17$ ns). The γ-rays from the decay of the state near 580 and

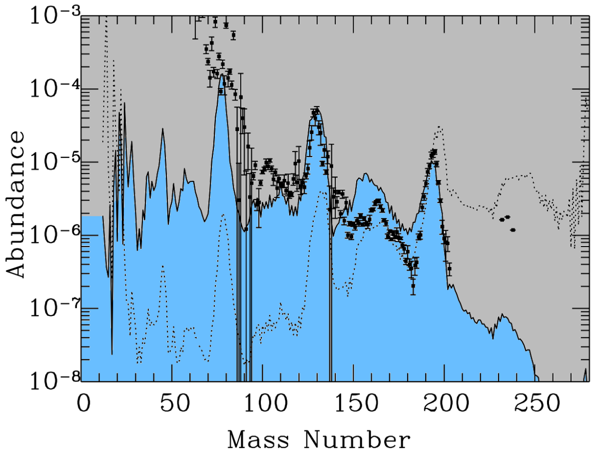

Figure 3: *Abundances of the various isotopes, calculated in [12] using a restricted network of reaction (dashed line) or full (plain line) network of reactions compared to experimental values.*

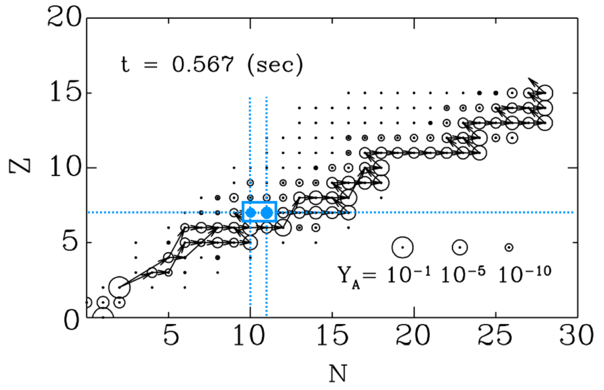

Figure 4: *Abundances of light nuclei at a specific time scale of a type II supernovae explosion. The reaction of interest,* ^{17}*N(n,*γ*)*^{18}*N is highlighted in blue.*

740 keV should allow the energies of the separate states in each doublet to be determined. Note that the γ-decay pathway for the different spins will be quite different. It should also be noted that the differential cross sections will be very different for the two members of each doublet. For example the 3^- at 742 keV will have *d*-wave transfer and the 1^- at 747 keV has *s*-wave transfer. Therefore, the 3^- differential cross section will be greatest nearer to 90° in the laboratory frame and the 1^- differential cross section will be greatest closer to 180° in the laboratory.

We should not rule out the possibility that the (d,p) transfer will populate positive parity bound states as well. They would be populated through admixtures of $\nu(1p_{3/2})$ and $\nu(1p_{1/2})$ configurations. According to the WBP shell model calculation presented here, which incidentally fails to predict the energies correctly for either negative or positive parity states, the spectroscopic factors for the positive parity states are very small. However, these same calculations predict that the lowest $(0p)^{-1}$ neutron states $(\frac{1}{2}^-,\frac{3}{2}^-)$ in ^{19}O should not be seen in (d,p), whereas experimentally the admixtures of $\nu(1p_{3/2})$ and $\nu(1p_{1/2})$ are sufficient that the lowest states are easily measured [15].

In summary, the (d,p) transfer measurements provide a unique opportunity to disentangle the details of the ^{18}N structure, and also a unique opportunity to measure the spectroscopic strengths required for the astrophysical application to element synthesis in supernovae. In the case of the positive parity states, the present ^{17}N(d,p) measurement should allow a limit to be set, at least, on the contributions from positive parity states to the (n,γ) astrophysical process. This is important, because the direct neutron capture into such states is not inhibited by any centrifugal barrier. The capture can be via direct E1 capture from the *s*-wave continuum, into a *p*-wave orbital in ^{18}N.

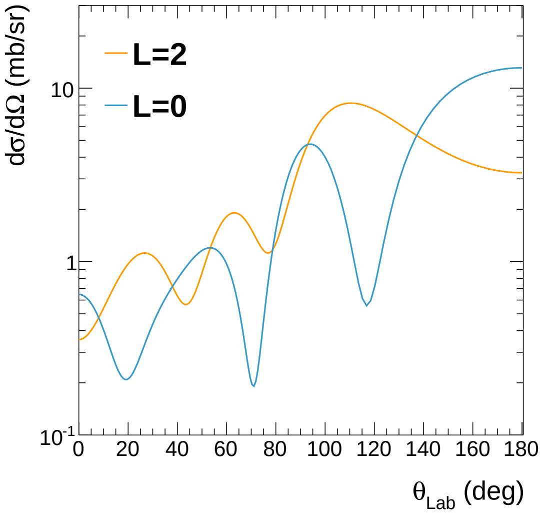

Figure 5: *ADWA cross sections in the laboratory frame with zero range approximation assuming S=1: (a) L=2, 742 keV* 3^-*, and (b) L=0, 745 keV* 1^-*.* E_{beam}*=5.5 AMeV*

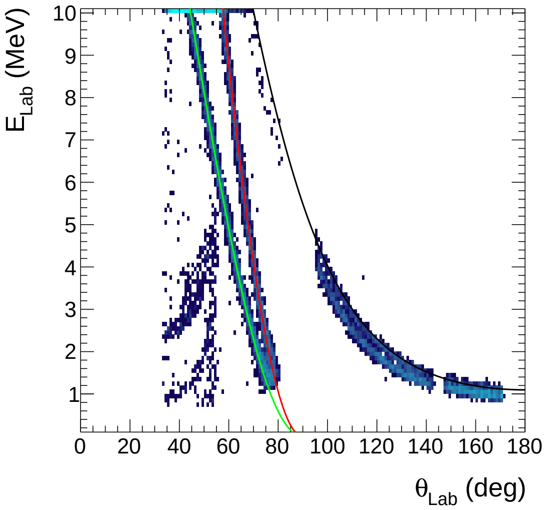

Figure 6: *Kinematic lines at 5.5 AMeV plotted over the Geant4 simulation. Black: (d,p) line for* $^{18}N_{g.s.}$*. Red:* $^{17}N(d,d)$ *. Green:* $^{17}N(p,p)$

3 Theoretical analysis of the ^{17}N(n,γ)^{18}N reaction

The present proposal will benefit from the close interaction and collaboration with reaction theorists. The measured angular distributions will be analysed using the latest developments in the theory of (d,p) reactions published in ref.[16]. These developments are based on non-local interactions of nucleons in deuteron with the target and an ongoing program of further development of these ideas is being pursued by the Nuclear Theory Group at the University of Surrey. The latest theory extends the adiabatic distorted wave approximation (ADWA) of Johnson and Soper. For a preliminary estimation of the reaction yields, in order to calculate the beam time requirements, we have performed ADWA calculations of d(^{17}N,p)^{18}N and these are shown in Fig. 5.

4 Experimental setup

The T-REX detector allows the detection of the proton from the (d,p) reaction at backward angles using four 500μm silicon box detectors and a complete 500μm annular detector. The Si segmentation is sufficient to achieve an acceptable resolution in excitation energy. In order to resolve the closely spaced states in ^{18}N we plan to measure the γ-rays coming from the beam-like ejectile, using the Miniball array. We assume an efficiency of 5% at 1.3 MeV [17]. Doppler shift corrections will be applied. In addition, we plan to use the forward box detector of T-REX, comprising four telescopes of 140 μm ΔE and 500 μm E, in order to measure the elastic scattering of the beam on both protons and deuterons in the target. This measurement allows an accurate normalisation of the measured differential cross section in the transfer channel.

We plan to employ a device such as the Trifoil detector in the beam at zero degrees, beyond the target chamber. Immediately in front of the trifoil, the use of an appropriate thickness of aluminium, typically a few tens of micrometers, allows the products from compound nuclear reactions to be stopped, and lets the beam and transfer reaction products pass. The Trifoil then comprises a 10 μm thick plastic scintillator foil coupled to three photomultipliers. In use with beams of 5 MeV/A at TRIUMF [4] this layout has proven to be essential to eliminate background in the gamma ray spectra and suppress a large part of the carbon induced background in the proton spectra (improving signal to background ratio by an order of magnitude).

Detector	Reaction	θ_{Lab}	Thickness
QQQ2	(d,p)	5-35°	500μm
X1	(d,p)	25-80°	500μm
X1	(d/p,d/p)	100-155°	140μm-500μm
QQQ2/1*	(d,^{3}He/t)	145-175°	140μm-500μm

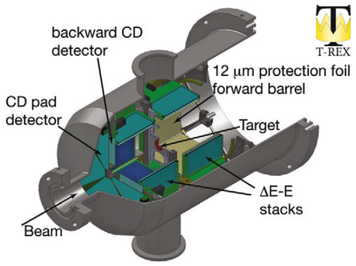

Table 2: *Layout of the detection for the T-REX array. Detectors marked with an asterisk are optional. Engineering drawing taken from [17]*

5 Beam time requirement

According to the yield data base of the Isolde facility we assume a production rate of ^{17}N at 10^5 pps using a CaO target. Following the guide line for beam intensity we estimate an efficiency of 10% for the Trap+EBIS+ REX mass separator, giving around 10^4 pps on the reaction target. The estimated counts for 7 days of full beam time, using a 0.5 mg/cm^2 thick CD_2 target can be found in Tab.4. According to this estimate, it is necessary to run for a total of 7 days on the (d,p) reaction, giving a required time of 10 days in total, allowing enough time for beam tuning and optimisation of the experimental apparatus. The expected energy resolution and detected count rate are estimated from a Geant4 simulation taking into account the target thickness and the geometry of the detection setup, as well as the angular distribution. The estimated count rate gives us confidence in our ability to extract useful angular distributions for the states with spectroscopic factors greater than 0.1. The gamma-rays can be used for gating, subject to statistics, but in any case will define very accurately the energies of states and their relative intensities, as for example was done in ref. [1].

Summary of requested shifts: We are requesting 30 shifts of ^{17}N beam at 5.5 MeV/A and 10^4 pps on the reaction target. The beam should be delivered at the T-REX + Miniball setup. We have initiated a liaison with the spokespersons of T-REX regarding this proposal.

E (keV)	J^π	ℓ	S	$\sigma_{DWBA}(mb)$	Total count	Count per 1° bin	FWHM (keV)
0	1^-	2	0.01	15.14	10	0-1	275
121	2^-	2	0.70	28.91	1050	10-25	350
580	0^-	0	0.71	11.84	350	5-30	430
742	3^-	2	0.69	47.20	1650	20-40	360
747	1^-	0	0.71	34.85	1050	10-50	450

Table 3: *Expected counting rates and resolutions for states populated via* $^{17}N(d,p)^{18}N$.

Beam	Min.Intensity	Target Material	Ion Source	Shifts
^{17}N	1.10^4	nano-CaO	Helicon	30

Table 4: *Summary of the beam production informations*

References

[1] W.N. Catford *et al.* *Phys. Rev. Lett.*, 104:192501, 2010.

[2] S. M. Brown *et al.* *Phys. Rev. C*, 85:011302, 2012.

[3] B. Fernández-Domínguez *et al.* *Phys. Rev. C*, 84:011301, 2011.

[4] G. L. Wilson *et al.* Ph.d. thesis. *Surrey, 2012, and in preparation for PRC*, 2012.

[5] M. Freer *et al.* *Phys. Rev. Lett.*, 82:1383–1386, 1999.

[6] B. Fernández-Domínguez and W.N. Catford. *GANIL Experiment E628*, 2011.

[7] M. Assie *et al.* *Int. J. Mod. Phys. E*, 20:971, 2011.

[8] G.D. Putt *et al.* *Nuclear Physics A*, 399(1):190 – 198, 1983.

[9] Brookhaven data base. *www.nndc.bnl.gov/nudat2/getdataset.jsp?nucleus=18N.*

[10] F.C. Barker. *Australian Journal of Physics*, 37:17–22, 1984.

[11] B.A. Brown and W.D.M. Rae. Nushell@msu. *MSU-NSCL Report, 2007.*

[12] M. Terasawa *et al.* *The Astrophysical Journal*, 562(1):470, 2001.

[13] T. Sasaqui *et al.* *The Astrophysical Journal*, 634(2):1173, 2005.

[14] H. Herndl *et al.* *Phys. Rev. C*, 60:064614, Nov 1999.

[15] S.Sen *et al.* *Nucl.Phys. A*, 219:429, 1974.

[16] N.K. Timofeyuk and R.C. Johnson. *Phys. Rev. Lett.*, 110:112501, 2013.

[17] V. Bildstein *et al.* *The European Physical Journal A*, 48(6):1–10, 2012.

Appendix

DESCRIPTION OF THE PROPOSED EXPERIMENT

The experimental setup comprises: MINIBALL + T-REX

Part of the	Availability	Design and manufacturing
MINIBALL + T-REX	☒ Existing	☒ To be used without any modification
[Part 1 of experiment/ equipment]	☐ Existing	☐ To be used without any modification ☐ To be modified
	☐ New	☐ Standard equipment supplied by a manufacturer ☐ CERN/collaboration responsible for the design and/or manufacturing
[Part 2 of experiment/ equipment]	☐ Existing	☐ To be used without any modification ☐ To be modified
	☐ New	☐ Standard equipment supplied by a manufacturer ☐ CERN/collaboration responsible for the design and/or manufacturing
[insert lines if needed]		

HAZARDS GENERATED BY THE EXPERIMENT (if using fixed installation:) Hazards named in the document relevant for the fixed MINIBALL + T-REX installation.

Additional hazards:

Hazards	[Part 1 of experiment/ equipment]	[Part 2 of experiment/ equipment]	[Part 3 of experiment/ equipment]
Thermodynamic and fluidic			
Pressure	[pressure][Bar], [volume][l]		
Vacuum			
Temperature	[temperature] [K]		
Heat transfer			
Thermal properties of materials			
Cryogenic fluid	[fluid], [pressure][Bar], [volume][l]		
Electrical and electromagnetic			
Electricity	[voltage] [V], [current][A]		
Static electricity			
Magnetic field	[magnetic field] [T]		
Batteries	☐		
Capacitors	☐		
Ionizing radiation			

Target material [material]			
Beam particle type (e, p, ions, etc)			
Beam intensity			
Beam energy			
Cooling liquids	[liquid]		
Gases	[gas]		
Calibration sources:	☐		
• Open source	☐		
• Sealed source	☐ [ISO standard]		
• Isotope			
• Activity			
Use of activated material:			
• Description	☐		
• Dose rate on contact and in 10 cm distance	[dose][mSV]		
• Isotope			
• Activity			
Non-ionizing radiation			
Laser			
UV light			
Microwaves (300MHz-30 GHz)			
Radiofrequency (1-300 MHz)			
Chemical			
Toxic	[chemical agent], [quantity]		
Harmful	[chem. agent], [quant.]		
CMR (carcinogens, mutagens and substances toxic to reproduction)	[chem. agent], [quant.]		
Corrosive	[chem. agent], [quant.]		
Irritant	[chem. agent], [quant.]		
Flammable	[chem. agent], [quant.]		
Oxidizing	[chem. agent], [quant.]		
Explosiveness	[chem. agent], [quant.]		
Asphyxiant	[chem. agent], [quant.]		
Dangerous for the environment	[chem. agent], [quant.]		
Mechanical			

Physical impact or mechanical energy (moving parts)	[location]		
Mechanical properties (Sharp, rough, slippery)	[location]		
Vibration	[location]		
Vehicles and Means of Transport	[location]		
Noise			
Frequency	[frequency],[Hz]		
Intensity			
Physical			
Confined spaces	[location]		
High workplaces	[location]		
Access to high workplaces	[location]		
Obstructions in passageways	[location]		
Manual handling	[location]		
Poor ergonomics	[location]		

Hazard identification:

Average electrical power requirements (excluding fixed ISOLDE-installation mentioned above):
Nothing additional to the standard setup of T-REX and MINIBALL.